

Global failure probability function estimation based on an adaptive strategy and combination algorithm

Xiukai Yuan^{a,*}, Yugeng Qian^a, Jingqiang Chen^a, Matthias G.R. Faes^{b,**}, Marcos A. Valdebenito^b, Michael Beer^{d,e,f}

^a*School of Aerospace Engineering, Xiamen University, Xiamen 361005, P. R. China*

^b*Chair for Reliability Engineering, TU Dortmund University, Leonhard-Euler-Strasse 5, 44227 Dortmund, Germany.*

^c*Institute for Risk and Reliability, Leibniz Universität Hannover, Callinstr. 34, Hannover, Germany*

^d*Institute for Risk and Uncertainty, University of Liverpool, Peach Street, L69 7ZF Liverpool, United Kingdom*

^e*International Joint Research Center for Resilient Infrastructure & International Joint Research Center for Engineering Reliability and Stochastic Mechanics, Tongji University, Shanghai 200092, China*

Abstract

1 The failure probability function (FPF) expresses the probability of failure as a function of the
2 distribution parameters associated with the random variables of a reliability problem. Knowledge
3 on this FPF is of much relevance for reliability sensitivity analysis and reliability-based design op-
4 timisation. However, its calculation is usually a challenging task. Therefore, this paper presents
5 an efficient approach for estimating the FPF based on on an adaptive strategy and a combina-
6 tion algorithm. The proposed approach involves three basic elements: 1) a Weighted Importance
7 Sampling approach, which allows determining local FPF estimates; 2) an adaptive strategy for
8 determining at which realisations of the distribution parameters it is necessary to perform lo-
9 cal FPF estimation; and 3) an optimal combination algorithm, which allows to aggregate local
10 FPF estimations together to form a global estimate of the FPF. Test and practical examples are
11 presented to demonstrate the efficiency and feasibility of the proposed approach.

Keywords: Failure probability function, Importance Sampling, Combination algorithm,
Adaptive strategy

1. Introduction

12 Recent advances in computational mechanics allow to explicitly model the unavoidable effects
13 of uncertainty on the performance of engineering systems [1]. Typically, one is interested in
14 assessing the reliability of the system through metrics such as the failure probability, including
15 either its sensitivity [2] or even optimising the system's design considering its level of reliability [3].
16 In all of the aforementioned cases, it is of importance to determine the relation between the

17 probability of failure and the distribution parameters associated with the random variables of a
18 reliability problem. Such relation has been termed in the literature as the Failure Probability
19 Function (FPF). The main objective of this work is to propose an efficient numerical procedure
20 for approximating this FPF.

21 The current approaches for FPF estimation can be roughly grouped into three classes. The first
22 class comprises surrogate modelling approaches. In essence, a surrogate models involves selecting
23 some predefined interpolation points in the space of the distribution parameters by means of design
24 of experiments. Then, reliability analyses are carried on these interpolation points, allowing
25 to train the surrogate model. For example, Gasser [4] adopts a predefined quadratic function
26 to approximate the logarithm of FPF. Jensen [5] adopted a linear function to approximate the
27 logarithm of FPF. Note that other types of surrogate model methods such as Kriging [6, 7], Support
28 vector machine [8, 9], etc., which are widely applied in reliability analysis to approximate the limit
29 state function [10, 11], can be also used to approximate the FPF. The second class of approaches
30 provides a *local* approximation of the FPF with respect to distribution parameters by performing
31 a standard reliability analysis. In this context, *local* implies that the approximation of the FPF is
32 valid over a small neighbourhood around an expansion point. For example, Zou and Mahadevan
33 [12] expressed the FPF as a linear function of the distribution parameters by applying a first-
34 order Taylor series about an expansion point based on reliability sensitivity information. Yuan
35 [13] proposed a weighted approach to obtain the FPF. In the latter approach, the estimate of FPF
36 is expressed as a function of a set of samples of the distribution parameters which are generated
37 in a single reliability analysis. Further, an advanced Line sampling approach is proposed to solve
38 the FPF in [14], which is similar to the weighted approach, as it only needs one simulation run of
39 Line Sampling. The third class of strategies for estimating the FPF involves the formulation of
40 the reliability problem in an augmented space. The seminal work of Au [15] proposes to calculate
41 the FPF by using the Bayes' rule and a single augmented reliability analysis. In this context,
42 *augmented* implies that distribution parameters are modelled as random variables. Naturally,
43 this is just a convenient artefact that allows applying the Bayes' rule. Ching and Hsieh [16, 17]
44 follow the augmented reliability idea and adopted the maximum entropy principle to estimate the
45 posterior distribution associated with distribution parameters. Taflanidis and Beck [18] perform
46 minimisation of the FPF in the augmented space by means of stochastic search. Feng et al. [19]
47 investigates the application of augmented space in conjunction with a binning algorithm. Ling et

48 al. [20] also apply the augmented space idea, and combine adaptive Kriging with Monte Carlo
49 simulation to estimate the FPF. Yuan and coworkers [21] further developed the aforementioned
50 concept to estimate the FPF with respect to distribution parameters by sample average which
51 can relieve the distribution fitting step. Zhang et al. [22] proposed an ensemble model method
52 based on Bayes' rule and augmented theory for estimating the FPF by using a weighted form to
53 combine numerous surrogate models.

54 As noted from the above discussion, approximating the FPF has been a topic of active re-
55 search. Despite all progresses made, there are still open issues which require further research. For
56 example, the first class of methods produces an approximation of the FPF estimator without ad-
57 ditional information regarding its precision. The second class of methods actually provides a local
58 approximation of FPF, which may lack accuracy for some problems, especially when the design
59 space associated with the distribution parameters is large. Finally, the third class of methods
60 may not be suitable for problems which involve a considerable number of distribution parame-
61 ters. Therefore, in this contribution, a *global* FPF estimation based on Adaptive strategy and
62 Combination algorithm (AC) is proposed. AC consists of the following three key elements.

- 63 1. The weighted approach developed in [13] is adopted as fundamental simulation tool to obtain
64 a local approximation of the FPF about specified values of distribution parameters.
- 65 2. An optimal combination algorithm is proposed to aggregate local FPF estimations together
66 to form the global FPF estimator.
- 67 3. An adaptive strategy is proposed to actively determine the values of distribution parameters
68 at which the local FPF estimation is carried out. This adaptive strategy is actually an active
69 search which seeks to minimise an error measure.

70 Note that it is worth pointing out the differences between the proposed approach with various
71 Importance Sampling (IS) methods. It has been observed in [20, 23] that most IS methods
72 address the computation of failure probability for specific values of the distribution parameters
73 of a reliability problem. Weighted Importance Sampling (WIS) [13] extends the traditional IS
74 approach by introducing an instrumental IS density function that admits a range of values for the
75 distribution parameters of a reliability problem. In that way, it is possible to determine a closed-
76 form estimator for the FPF. However, WIS is typically a local approximation method. Therefore,
77 the adaptive strategy and an optimal combination algorithm proposed in this work allow to extend
78 its capability from local estimation to global estimation. In this sense, the proposed approach can

79 be seen as an extended version of the weighted approach reported in [13].

80 This contribution is organised as follows. In Section 2, the formal definition of FPF estimation
81 is briefly presented. Then, the mathematical formulation of the proposed framework is developed
82 in Section 3. In Section 4, various examples are presented to show the performance of the proposed
83 approach. Finally, Section 5 lists the conclusions of the paper.

84 2. Problem definition

85 The objective of this contribution is calculating failure probability as a function of distribution
86 parameters associated with the random variables of a reliability problem. This is termed as
87 failure probability function (FPF) and is denoted as $P_F(\boldsymbol{\theta})$, where P_F denotes failure probability;
88 $\boldsymbol{\theta} = [\theta_1, \dots, \theta_{n_\theta}] \in \mathcal{S}$ is the vector of distribution parameters and \mathcal{S} the hyper-rectangular design
89 space to which the distribution parameters belong to. Note that \mathcal{S} is bounded either by the
90 physics of the problem under consideration or by a priori considerations. In addition, note that
91 the vector of distribution parameters $\boldsymbol{\theta}$ can be also interpreted as a design vector [3].

92 The failure probability function $P_F(\boldsymbol{\theta})$ is defined as:

$$P_F(\boldsymbol{\theta}) = \int I_F(\mathbf{x})f(\mathbf{x} | \boldsymbol{\theta})d\mathbf{x}, \quad (1)$$

93 where \mathbf{x} is a vector-valued realisation of the random variable vector \mathbf{X} that characterises the
94 uncertain inputs of a reliability problem; $f(\mathbf{x} | \boldsymbol{\theta})$ is the PDF of \mathbf{X} conditioned on the distribution
95 parameters $\boldsymbol{\theta}$; and $I_F(\mathbf{x})$ is the indicator function, which assumes the value $I_F(\mathbf{x}) = 1$ if $\mathbf{x} \in F$ and
96 $I_F(\mathbf{x}) = 0$ otherwise. Note that F represents the failure domain associated with the realisations
97 of the random variable vector. It is defined as $F = \{\mathbf{x} : g(\mathbf{x}) < 0\}$, where $g(\mathbf{x})$ is the performance
98 function, which assumes a value equal or smaller than zero in case that the realisation \mathbf{x} of the
99 uncertain input parameters causes an unacceptable system's behaviour. Inspection of the above
100 equation indeed reveals that, in order to fully map $P_F(\boldsymbol{\theta})$, a full reliability analysis is required for
101 each $\boldsymbol{\theta} \in \mathcal{S}$.

102 3. Proposed approach for global FPF estimation

103 3.1. Overview of the proposed approach

104 This section presents the proposed approach to estimate the FPF efficiently with high global
105 accuracy, which is based on an adaptive strategy and a combination algorithm. The global FPF

106 estimator $\hat{P}_{F,C}^{(k)}(\boldsymbol{\theta})$ is obtained by combining a number of k local estimators, and is explicitly given
 107 by:

$$\hat{P}_{F,C}^{(k)}(\boldsymbol{\theta}) = \sum_{i=1}^k w_i(\boldsymbol{\theta}) \hat{P}_F^{(i)}(\boldsymbol{\theta}), \quad (2)$$

108 where $\hat{P}_F^{(i)}(\boldsymbol{\theta})$ is the i -th local estimator, whose calculation is explained in detail in Section 3.2;
 109 k is the total number of different local estimators; and $w_i(\boldsymbol{\theta})$ is a weight function. Note that
 110 $\sum_{i=1}^k w_i(\boldsymbol{\theta}) = 1$ is imposed for each value of $\boldsymbol{\theta}$. Thus, as long as $\hat{P}_F^{(i)}(\boldsymbol{\theta})$ is unbiased, then the
 111 obtained $\hat{P}_{F,C}^{(k)}(\boldsymbol{\theta})$ is also unbiased. The exact values of each $w_i(\boldsymbol{\theta})$ are obtained via a combination
 112 algorithm, as explained in detail in Section 3.3. Furthermore, the identification of the realisations
 113 of $\boldsymbol{\theta}$ at which a local FPF estimator is required is carried out by means of active learning, as
 114 described in detail in Section 3.4.

115 Before continuing, it is useful to derive some properties of the global FPF estimator shown
 116 in Eq. 2. In case that the FPF components, $\hat{P}_F^{(i)}(\boldsymbol{\theta})$, are mutually independent, the variance of
 117 $\hat{P}_{F,C}^{(k)}(\boldsymbol{\theta})$ can be easily obtained by

$$\text{Var} \left[\hat{P}_{F,C}^{(k)}(\boldsymbol{\theta}) \right] = \sum_{i=1}^k w_i^2(\boldsymbol{\theta}) \text{Var} \left[\hat{P}_F^{(i)}(\boldsymbol{\theta}) \right] \quad (3)$$

118 Further, if all the FPF components, $\hat{P}_F^{(i)}(\boldsymbol{\theta})$, are unbiased estimators, i.e., $E[\hat{P}_F^{(i)}(\boldsymbol{\theta})] = P_F(\boldsymbol{\theta})$,
 119 then the coefficient of variation (C.o.V.) of $\hat{P}_{F,C}^{(k)}(\boldsymbol{\theta})$ is given by

$$\text{Cov}[\hat{P}_{F,C}^{(k)}(\boldsymbol{\theta})] = \frac{\sqrt{\sum_{i=1}^k w_i(\boldsymbol{\theta})^2 \text{Var}[\hat{P}_F^{(i)}(\boldsymbol{\theta})]}}{P_F(\boldsymbol{\theta})} = \sqrt{\sum_{i=1}^k w_i^2(\boldsymbol{\theta}) \text{Cov}^2[\hat{P}_F^{(i)}(\boldsymbol{\theta})]} \quad (4)$$

120 3.2. Local estimate of FPF by the weighted approach

121 A local estimate of the FPF is produced by means of the Weighted Importance Sampling
 122 (WIS) approach presented in [13]. The first step of WIS consists of introducing an instrumental
 123 probability density function $H(\mathbf{x})$. Then, the FPF in Eq. (1) is rewritten as:

$$P_F(\boldsymbol{\theta}) = \int \frac{I_F(\mathbf{x}) f(\mathbf{x} | \boldsymbol{\theta})}{H(\mathbf{x})} H(\mathbf{x}) d\mathbf{x} \quad (5)$$

124 which is further expressed as:

$$P_F(\boldsymbol{\theta}) = E_H \left[\frac{I_F(\mathbf{x}) f(\mathbf{x} | \boldsymbol{\theta})}{H(\mathbf{x})} \right] = E_H [I_F(\mathbf{x}) r(\mathbf{x}, \boldsymbol{\theta})] \quad (6)$$

125 where $r(\mathbf{x}, \boldsymbol{\theta}) = f(\mathbf{x} | \boldsymbol{\theta})/H(\mathbf{x})$ is the ratio of two distributions. Assume that N samples are
 126 generated according to $H(\mathbf{x})$, that is, $\{\mathbf{x}^{(j)}, j = 1, \dots, N\}$. Then, the FPF can be estimated as:

$$\hat{P}_F(\boldsymbol{\theta}) = \frac{1}{N} \sum_{j=1}^N \frac{I_F(\mathbf{x}^{(j)}) f(\mathbf{x}^{(j)} | \boldsymbol{\theta})}{H(\mathbf{x}^{(j)})} \quad (7)$$

127 The above equation provides a generic expression for the local approximation of the FPF
 128 produced by means of Weighted Importance Sampling. For the i -th ($i = 1, 2, \dots, k$) local
 129 estimator of the FPF, an Importance Sampling Density (ISD) function $H(\mathbf{x})$ is established around
 130 the support point $\boldsymbol{\theta}_H^{(i)}$. Specifically, the so-called ISD based on the design point [24] is considered
 131 here, which is given as:

$$H(\mathbf{x}) = H(\mathbf{x} | \mathbf{x}^{*(i)}) \quad (8)$$

132 where $\mathbf{x}^{*(i)}$ is the design point solved according to the current support parameter point $\boldsymbol{\theta} = \boldsymbol{\theta}_H^{(i)}$,
 133 that is, when \mathbf{x} is distributed as $f(\mathbf{x} | \boldsymbol{\theta}_H^{(i)})$.

134 Suppose that a number of $N^{(i)}$ samples are generated according to $H(\mathbf{x} | \mathbf{x}^{*(i)})$, i.e., $\{\mathbf{x}^{(j)} \sim$
 135 $H(\mathbf{x} | \mathbf{x}^{*(i)}), j = 1, \dots, N^{(i)}\}$. According to Eq. (6), $P_F(\boldsymbol{\theta})$ can be estimated based on these
 136 samples by

$$\hat{P}_F^{(i)}(\boldsymbol{\theta}) = \frac{1}{N} \sum_{j=1}^N \frac{I_F(\mathbf{x}^{(j)}) f(\mathbf{x}^{(j)} | \boldsymbol{\theta})}{H(\mathbf{x}^{(j)} | \mathbf{x}^{*(i)})} \quad (9)$$

137 Obviously, the estimator in Eq. (9) is unbiased for each value of $\boldsymbol{\theta}$. The corresponding variance
 138 and coefficient of variation are given by

$$Var[P_F^{(i)}(\boldsymbol{\theta})] \approx \frac{1}{N-1} \left\{ \frac{1}{N} \sum_{j=1}^N \left[\frac{I_F(\mathbf{x}^{(j)}) f(\mathbf{x}^{(j)} | \boldsymbol{\theta})}{H(\mathbf{x}^{(j)} | \mathbf{x}^{*(i)})} \right]^2 - [\hat{P}_F^{(i)}(\boldsymbol{\theta})]^2 \right\} \quad (10)$$

$$Cov[P_F^{(i)}(\boldsymbol{\theta})] = \frac{\sqrt{Var[\hat{P}_F^{(i)}(\boldsymbol{\theta})]}}{P_F(\boldsymbol{\theta})} \approx \frac{\sqrt{Var[\hat{P}_F^{(i)}(\boldsymbol{\theta})]}}{\hat{P}_F^{(i)}(\boldsymbol{\theta})} \quad (11)$$

139 The local estimate of FPF in Eq. (9) provides sufficient accuracy when $\boldsymbol{\theta}$ is near the current
 140 support parameter point $\boldsymbol{\theta}_H^{(i)}$. However, it may show a large coefficient of variation for values of
 141 $\boldsymbol{\theta}$ far from $\boldsymbol{\theta}_H^{(i)}$. The latter is undesirable, as it may imply considerable error in the prediction
 142 of the FPF and can be particularly problematic for large design spaces \mathcal{S} . Such issue can be
 143 circumvented by means of a combination algorithm, which is explained in the following.

144 *3.3. Combination algorithm*

145 An optimal Combination algorithm is proposed to determine the weights function $w_i(\boldsymbol{\theta})$ in
 146 Eq. (2). Note that the performance of Combination algorithm depends highly on the calculated
 147 weights, and hence, the approach used to calculate these weights is highly influential. There
 148 are three approaches for combination algorithm proposed in this paper: (1) equal weights; (2)
 149 determination of an optimal $w_i(\boldsymbol{\theta})$ that minimises the variance of $\hat{P}_{F,C}^{(i)}(\boldsymbol{\theta})$; and (3) determination
 150 of an optimal $w_i(\boldsymbol{\theta})$ that minimises the C.o.V. of $\hat{P}_{F,C}^{(i)}(\boldsymbol{\theta})$. These approaches are discussed and
 151 evaluated in the following.

152 *3.3.1. Combination based on average weights*

153 The most straightforward way to combine the local approximations of FPF is to add them
 154 considering equal weights, that is

$$w_i(\boldsymbol{\theta}) = \frac{1}{k} \quad (i = 1, \dots, k) \quad (12)$$

155 Generally, the combination based on average weights is quite easy to apply. However, it may
 156 provide poor estimates in other cases, as discussed later on.

157 *3.3.2. Optimal combination based on minimising the variance*

158 A set of optimal weights can be selected such that the variance of the FPF estimator $\hat{P}_{F,C}^{(k)}(\boldsymbol{\theta})$,
 159 as given in Eq. (2), is minimised. As explained in detail in Appendix A, the optimal weights that
 160 fulfill such criterion are:

$$w_i(\boldsymbol{\theta}) = \frac{Var^{-1}[\hat{P}_F^{(i)}(\boldsymbol{\theta})]}{\sum_{j=1}^k Var^{-1}[\hat{P}_F^{(j)}(\boldsymbol{\theta})]} \quad (i = 1, \dots, k) \quad (13)$$

161 This equation shows that the optimal weight associated with $\hat{P}_F^{(i)}(\boldsymbol{\theta})$ decreases with increase of
 162 the variance of $\hat{P}_F^{(i)}(\boldsymbol{\theta})$. Furthermore, substitution of Eq. (13) into Eq. (3), yields the variance of
 163 the estimate for the FPF, which is equal to

$$Var[\hat{P}_{F,C}^{(k)}(\boldsymbol{\theta})] = \frac{1}{\sum_{i=1}^k Var^{-1}[\hat{P}_F^{(i)}(\boldsymbol{\theta})]} \quad (14)$$

164 *3.3.3. Optimal combination based on minimising the C.o.V.*

165 The third approach consists of determining the weights such that $\hat{P}_{F,C}^{(k)}(\boldsymbol{\theta})$ possesses the smallest
 166 C.o.V. The optimal weights are then given by:

$$w_i(\boldsymbol{\theta}) = \frac{Cov^{-2}[\hat{P}_F^{(i)}(\boldsymbol{\theta})]}{\sum_{j=1}^k Cov^{-2}[\hat{P}_F^{(j)}(\boldsymbol{\theta})]} \quad (i = 1, \dots, k) \quad (15)$$

167 The detailed derivation of Eq. (15) is presented in Appendix A. Eq. (15) shows that the optimal
 168 weight of $\hat{P}_F^{(i)}(\boldsymbol{\theta})$ decreases with increase of the C.o.V. of $\hat{P}_F^{(i)}(\boldsymbol{\theta})$.

169 Furthermore, substitution of Eq. (15) into Eq. (4) yields the final C.o.V. of the estimate of
 170 FPF, which is equal to:

$$Cov[\hat{P}_{F,C}^{(k)}(\boldsymbol{\theta})] = \frac{1}{\sqrt{\sum_{i=1}^k Cov^{-2}[\hat{P}_F^{(i)}(\boldsymbol{\theta})]}} \quad (16)$$

171 Since $Cov[\hat{P}_F^{(i)}(\boldsymbol{\theta})] \neq 0$, thus $Cov[\hat{P}_F^{(i)}(\boldsymbol{\theta})]^2 > 0$, then it is easy to further deduce that:

$$Cov[\hat{P}_{F,C}^{(k)}(\boldsymbol{\theta})] \leq Cov[\hat{P}_F^{(i)}(\boldsymbol{\theta})], (i = 1, \dots, k) \quad (17)$$

172 which means that the combined estimate will own the smallest C.o.V. in theory compared with
 173 the local estimates of the FPF.

174 It should be noted that the optimal weights in Eqs. (13) and (15) depend on variance and co-
 175 variance, which are not available in closed form. In this case, the corresponding sample estimators
 176 could be used instead, but would introduce bias in the estimation, as discussed in [25]. However,
 177 the estimates presented in the paper are *biased but consistent*, which means that they will converge
 178 asymptotically to the correct value as the number of samples involved increases. This point is
 179 demonstrated through a lemma given in Appendix B and a test example in Subsection 4.1, which
 180 confirms that this effect is negligible for the purposes of this work.

181 3.3.4. Comparison of criteria for combination

182 A two-dimensional academic example is given to illustrate the three different combination
 183 criteria described previously. Suppose that the limit state function is given as $g(\mathbf{x}) = 4 - x_1 - x_2$,
 184 where $x_1 \sim N(\theta, 1)$, $x_2 \sim N(0, 1)$ are the basic random variables, and $\theta \in [-2, 2]$ is the distribution
 185 parameter for which the FPF is sought. Weighted Importance Sampling is applied twice, each
 186 time considering one of the following two design points: $\mathbf{x}_L^* = [1, 3]$ and $\mathbf{x}_U^* = [3, 1]$. It can be
 187 shown that these two are the design points when the distribution parameter is set as $\theta = -2$
 188 and $\theta = 2$, respectively. Each implementation of Weighted Importance Sampling (WIS) is carried
 189 out using $N = 100$ samples. The results by different settings and methods are plotted in Fig.
 190 1. In this figure, ‘WIS(\mathbf{x}_L^*)’ and ‘WIS(\mathbf{x}_U^*)’ denote the weighted approach with sampling centres
 191 on \mathbf{x}_L^* and \mathbf{x}_U^* , respectively; ‘Average weights’, ‘Variance weights’ and ‘C.o.V. weights’ denotes
 192 the combination based on average weights, minimising the variance of $\hat{P}_F^{(k)}(\boldsymbol{\theta})$ and the C.o.V. of
 193 $\hat{P}_F^{(k)}(\boldsymbol{\theta})$, respectively. Note that these combination estimators are constructed based on the two
 194 independent simulations of WIS, that is, $k = 2$.

195 It can be seen from Fig. 1 that the local FPF estimates obtained by means of WIS (that is,
 196 $\text{WIS}(\mathbf{x}_U^*)$ and $\text{WIS}(\mathbf{x}_L^*)$) can possess a large coefficient of variation. The approaches that combine
 197 the two local estimates of the FPF by means of weights exhibit a smaller coefficient of variation.
 198 Among these, the approach that uses weights that minimise the C.o.V exhibits the best accuracy.
 199 Based on this observation, in this work, only the combination algorithm based on minimising the
 200 C.o.V. is adopted and further investigated.

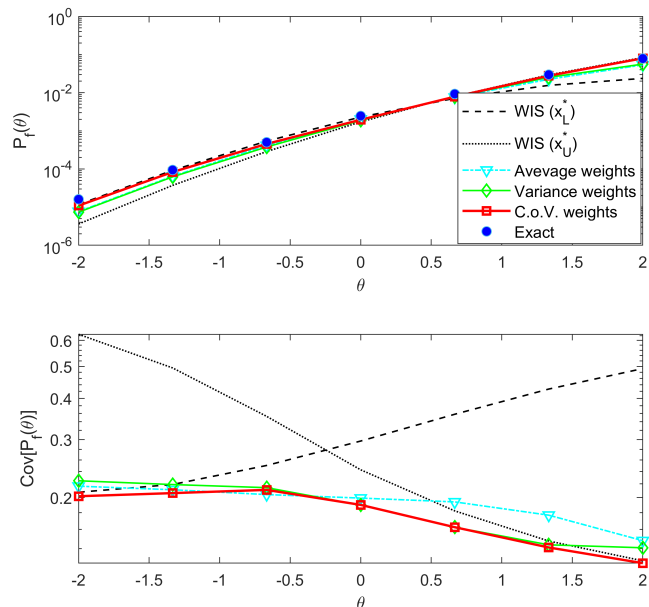


Figure 1: Comparison of the FPF estimators and C.o.V.'s by different ways.

201 3.4. Adaptive strategy

202 The above discussion has addressed the construction of a local estimate of the FPF (see Section
 203 3.2) as well as the aggregation of different local FPF into a combined estimator (see Section 3.3).
 204 Nonetheless, the issue on how to select the support point $\theta_H^{(i)}$ ($i = 2, 3, \dots, k$) for constructing a
 205 local approximation $\hat{P}_F^{(i)}(\theta)$ remains open. In principle, these support points can be selected a
 206 priori, e.g., through a predefined experimental design heuristics, like centre design, or following
 207 random approaches, such as MCS, Latin Hypercube Sampling (LHS) or other low-discrepancy
 208 sequences. However, such a priori experimental design may not be the most efficient approach.
 209 Hence, a novel way to determine the location of the support points associated with the construction
 210 of the local FPF estimators based on active learning is developed here. Since the C.o.V. is a good
 211 estimator of the precision of an estimator, the C.o.V. of the aggregated global FPF estimator

212 is used as a learning function to select the next support point for constructing a new local FPF
 213 estimate to augment (or improve) the quality of the current global estimate. Specifically, the point
 214 $\boldsymbol{\theta} \in \mathcal{S}$ that possesses the largest value of C.o.V. should be chosen as the next support point.

215 Suppose that the i -th estimator of the FPF $\hat{P}_{F,C}^{(i)}(\boldsymbol{\theta})$ is calculated according to Eq. (2), and
 216 the C.o.V. of the estimator is obtained according to Eq. (4), then the next support parameter
 217 point $\boldsymbol{\theta}_H^{(i+1)}$ is determined by solving the following optimisation problem:

$$\begin{aligned}
 &\text{Find } \boldsymbol{\theta}_H^{(i+1)} = \boldsymbol{\theta}_{\max} \\
 &\text{Max } Cov[\hat{P}_{F,C}^{(i)}(\boldsymbol{\theta})] \\
 &\text{s.t. } \underline{\theta}_j \leq \theta_j \leq \bar{\theta}_j \quad (j = 1, 2, \dots, n_\theta).
 \end{aligned} \tag{18}$$

218 where $\underline{\theta}_j$ and $\bar{\theta}_j$ denote the lower and upper bounds for θ_j . Note that this optimisation problem
 219 does not involve any evaluation of limit state function. Thus, it can be readily solved by adopting
 220 any appropriate optimisation algorithm. In this contribution, the optimisation problem in Eq. (18)
 221 is solved by means of MCS, as its implementation is quite straightforward. When the dimension
 222 of $\boldsymbol{\theta}$ is large (i.e., larger than 10), other algorithms, e.g., Particle Swarm Optimisation, can be
 223 used to solve Eq. (18).

224 Note that active strategy in Eq. (18) can be repeated, until convergence is reached. The
 225 stopping criterion can be selected as $\max(Cov[\hat{P}_F(\boldsymbol{\theta})]) \leq c_{tol}$, where c_{tol} is a given tolerance
 226 value.

227 3.5. Summary of the proposed approach

228 The proposed approach to estimate the global FPF in an active way can be summarised in
 229 the following steps, which are also depicted in a flow diagram in Fig. 2.

- 230 1. Initialise design. Set $i = 1$. Choose an initial value of $\boldsymbol{\theta}_H^{(1)}$. A possible choice is $\boldsymbol{\theta}_H^{(1)} =$
 231 $(\bar{\boldsymbol{\theta}} - \underline{\boldsymbol{\theta}})/2$, where $\bar{\boldsymbol{\theta}}$ and $\underline{\boldsymbol{\theta}}$ denote the maximum and minimum values that $\boldsymbol{\theta}$ may assume.
- 232 2. Carry out Weighted Importance Samplig (WIS). Based on the Importance Sampling density
 233 function, $H(\boldsymbol{x})$ given in Eq. (8) and the support point $\boldsymbol{\theta}_H^{(i)}$, produce samples $\{\boldsymbol{x}^{(j)} : j = 1, \dots, N\}$.
 234 The local FPF estimator is established by means of Eq. (9).
- 235 3. Produce the global FPF estimator with the optimal combination algorithm. Calculate the
 236 weights according to Eq. (15), and then produce the global FPF estimate following Eq. (2).
- 237 4. Determine the next support parameter point by active learning. Solve the optimisation
 238 problem in Eq. (18) to obtain next support parameter point $\boldsymbol{\theta}_H^{(i+1)}$.

239
240

5. In case that the maximum coefficient of variation of the global FPF estimate is above the tolerance c_{tol} , return to step 2 with $i = i + 1$. Otherwise, stop the iteration.

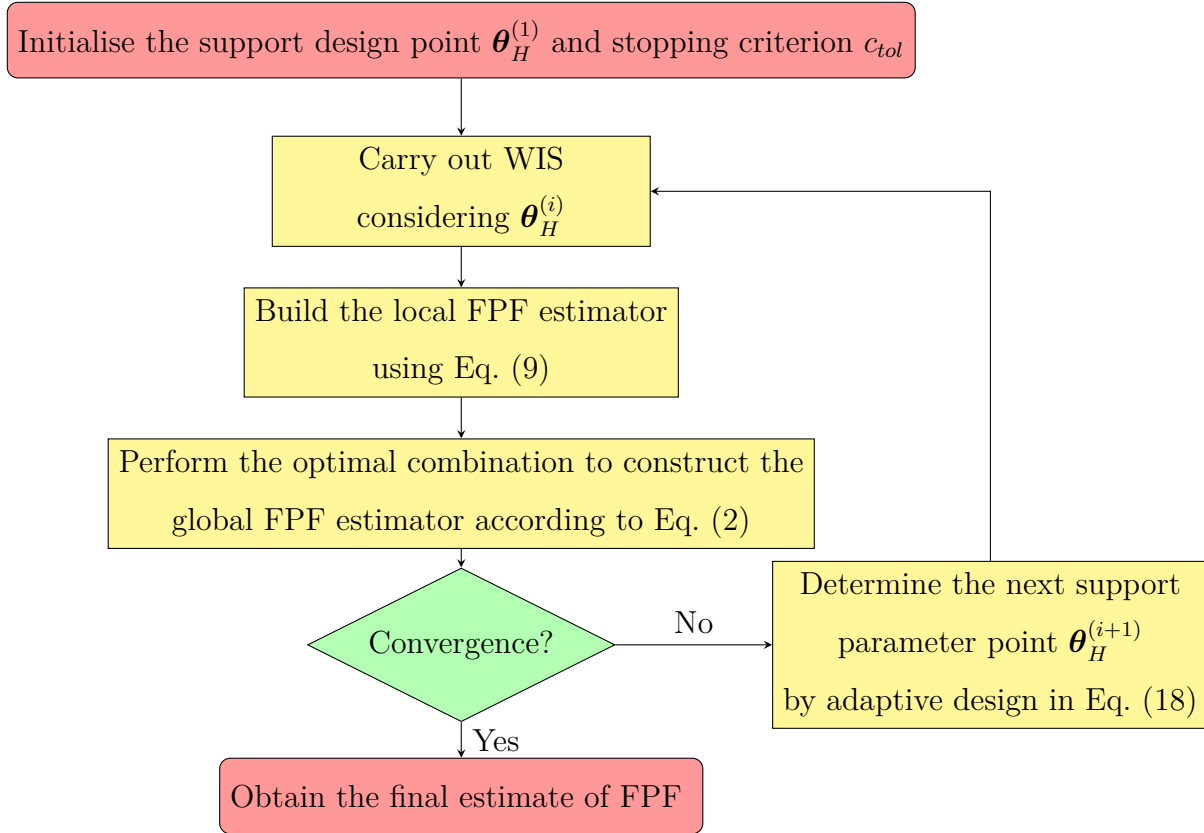


Figure 2: Flowchart of the proposed approach.

241 4. Examples

242 In this section, three examples are presented to illustrate the performance of the proposed
243 approach. These examples are solved by means of three different approaches:

- 244 (a) The proposed approach (which is denoted as AC) with weights selected such that the C.o.V.
245 of the global FPF estimate is minimised, as described in Section 3.3.3.
- 246 (b) The WIS approach, which corresponds to a local FPF estimation [13]. Note that this approach
247 is described in Section 3.2.
- 248 (c) An augmented space integral (ASI) approach implemented with Importance Sampling, as
249 proposed in [14]. It produces a global FPF estimation through reliability analysis in an
250 augmented reliability space.

251 Note that these selected approaches are comparable between them, as they are simulation-based
 252 methods where the corresponding C.o.V. of FPF is available. Note that methods based on response
 253 surface (or surrogate model) [5] or the augmented space method with density fitting [16] are not
 254 included in the comparison. Such decision is made as the latter methods require additional
 255 assumptions and they do not produce information on the C.o.V. of the probability estimates.
 256 Direct MCS and IS are also applied to obtain the point-wise values of failure probability which
 257 are regarded as the ‘exact values’. The optimisation problem in Eq. (18) is solved by random
 258 search using MCS. The stopping criterion $c_{tol} = 0.2$ is set for all the examples.

259 4.1. Example 1: A test example

260 The first example considers a simple limit state function, which is given by

$$g(\mathbf{x}) = 1 + \exp(-0.5x_1) - x_2 \quad (19)$$

261 where x_1 and x_2 are normal distributed random variables, i.e., $x_1 \sim N(\theta_1, 1)$ and $x_2 \sim N(\theta_2, 1)$,
 262 where the mean values of x_1 and x_2 are taken as the design parameters, and the design domains
 263 are $\theta_1 \in [-2.5, 2.5]$ and $\theta_2 \in [-2.5, 2.5]$.

264 4.1.1. Results of the proposed approach

265 The proposed approach is applied to estimate the global FPF of this problem. First $\theta_H^{(1)} =$
 266 $[-2.5, -2.5]$ is set, which is located in the lower bound of the design region. Then, the corre-
 267 sponding design point $\mathbf{x}^{*(1)} = [0.4851, 1.8646]$ is determined, and WIS based on this design point
 268 is performed with $N = 100$ samples. Note that the design point is solved by using Advance First
 269 Order and Second Moment (AFOSM) [26] method and 30 evaluations of the performance function
 270 are required.

271 Fig. 3 shows the two-dimensional FPF estimates obtained by the proposed method, as well
 272 as the two-dimensional C.o.V. of estimator. It can be seen that the final C.o.V. values are all
 273 less than 0.2. Further, Fig. 4a and 4b show two one-dimensional projections of the FPF, namely
 274 $P_F(\theta_1, \theta_2 = 0)$ and $P_F(\theta_1 = 0, \theta_2)$, with respect to the number of iterations, respectively. Direct
 275 MCS is applied with $N = 10^7$ samples for each point-wise value of FPF which is take as the ‘exact’
 276 value (denoted by ‘circle’). It can be seen that the FPF estimate is improved at each step of the
 277 iterative process. For example, in Fig. 4a, some error exists in the FPF estimator in the early
 278 steps, e.g., over the left and right sides of design region of θ_1 . The corresponding C.o.V.s are also

279 large. As the iteration process advances, the results are improved until the stopping criterion is
 280 reached.

281 In order to illustrate the effectiveness of the adaptive design, the C.o.V. of the estimator in
 282 each iteration, as well as the support parameter points $\theta_H^{(i)} (i = 1, \dots, 4)$ determined by the adaptive
 283 strategy, are shown in Fig. 5. The support points which are also the points with the biggest C.o.V.
 284 values in each iteration are shown in the figure (denoted by red dots). It can be noted that the
 285 C.o.V. of the estimator monotonically decreases as the iteration process continues.

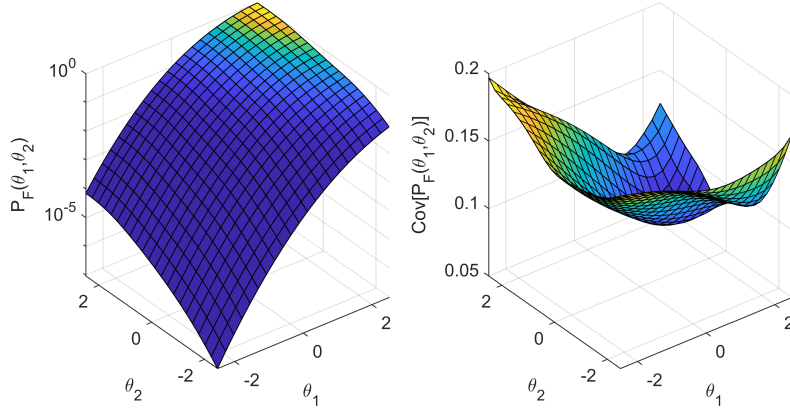
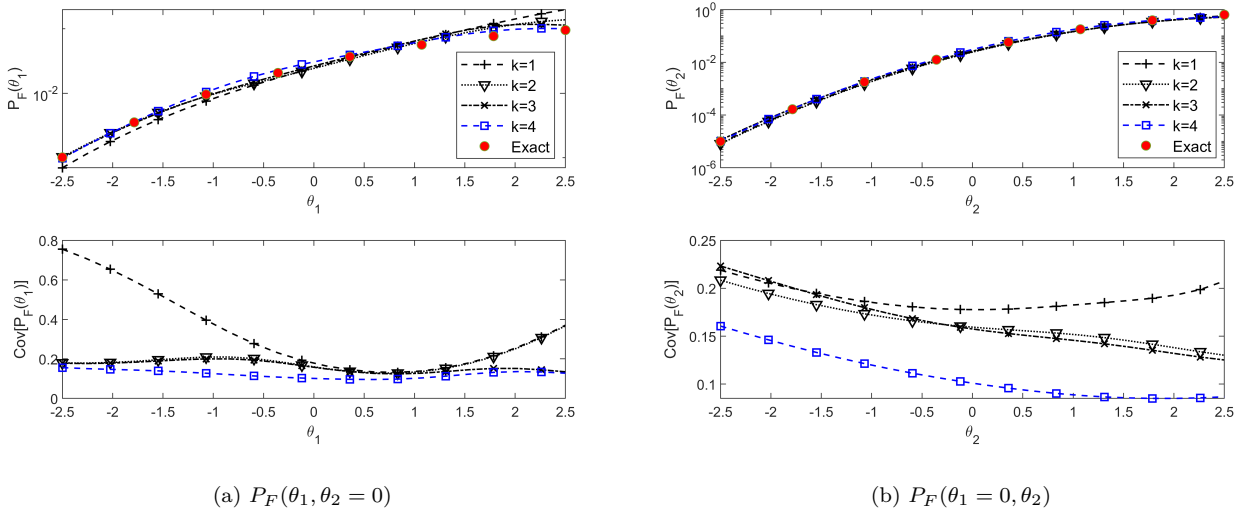


Figure 3: The FPF results by the proposed approach (Example 1).



(a) $P_F(\theta_1, \theta_2 = 0)$

(b) $P_F(\theta_1 = 0, \theta_2)$

Figure 4: The one-dimensional FPF results by the proposed method (Example 1).

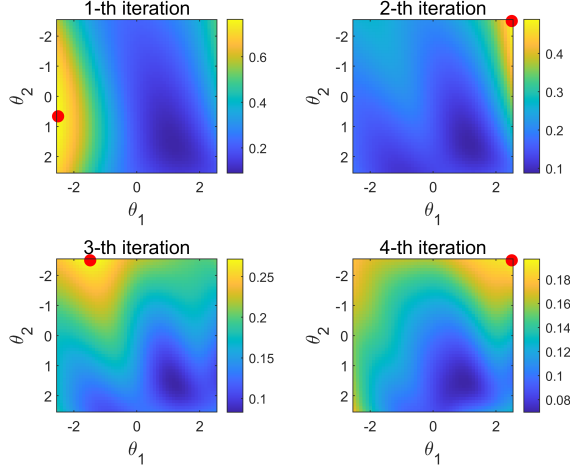


Figure 5: The C.o.V.s of the FPF results in each iteration by the proposed approach (Example 1). The red points denote the locations of $\boldsymbol{\theta}_H^{(k+1)}$ ($k = 1, \dots, 4$).

286 4.1.2. Comparison with other methods

287 The proposed method is compared with WIS and ASI in this subsection. First, all these
 288 methods are implemented with the same number of simulated samples, i.e., $N_T = N \times k = 100 \times 4$
 289 for the proposed approach, and $N = 400$ for the WIS and ASI-IS. The design point $\boldsymbol{x}^{*(1)}$ in
 290 the proposed approach is also used for WIS and ASI. Note that the computation cost of solving
 291 the design point is not included here since it is negligible compared to the limit state function
 292 evaluations in these approaches.

293 Fig. 6a and 6b shows the one dimensional FPF results (as well as their C.o.V. estimators). It
 294 can be seen in Fig. 6a that the FPF result of AC is consistent with the ‘Exact’ results by direct
 295 MCS, while those of both ASI and WIS possess considerable error when $\theta_1 \in [-2.5, -0.5]$. In both
 296 figures, ASI has the largest C.o.V. and also the proposed approach obtains the smoothest C.o.V.
 297 which owns the smallest maximum value of C.o.V. over the design region.

298 In addition, all these methods are implemented with the same stop criterion $Cov[\hat{P}_F(\boldsymbol{\theta})] \leq$
 299 $c_{tol} = 0.2$. Table 1 shows the total number of evaluations of the performance function (including
 300 the design points identification) by different methods through an average over 10 independent
 301 runs. Different initial support parameter points $\boldsymbol{\theta}_H^{(1)}$ are also considered, i.e., (1) initial design 1:
 302 $\boldsymbol{\theta}_H^{(1)} = [-2.5, -2.5]$, (2) initial design 2: $\boldsymbol{\theta}_H^{(1)} = [0, 0]$, and (3) initial design 3: $\boldsymbol{\theta}_H^{(1)} = [2.5, 2.5]$. It can
 303 be seen that the total number of evaluations of the performance function by WIS varies according
 304 to different starting points, i.e., from 5840 to 87100, while those of ASI-IS and are relatively
 305 steady. Among them, the proposed method based on an adaptive strategy and combination

306 algorithm (AC) requires the least number of calls to the performance function. This illustrates
 307 that, in this case, the proposed approach is more efficient and effective than WIS and ASI-IS.

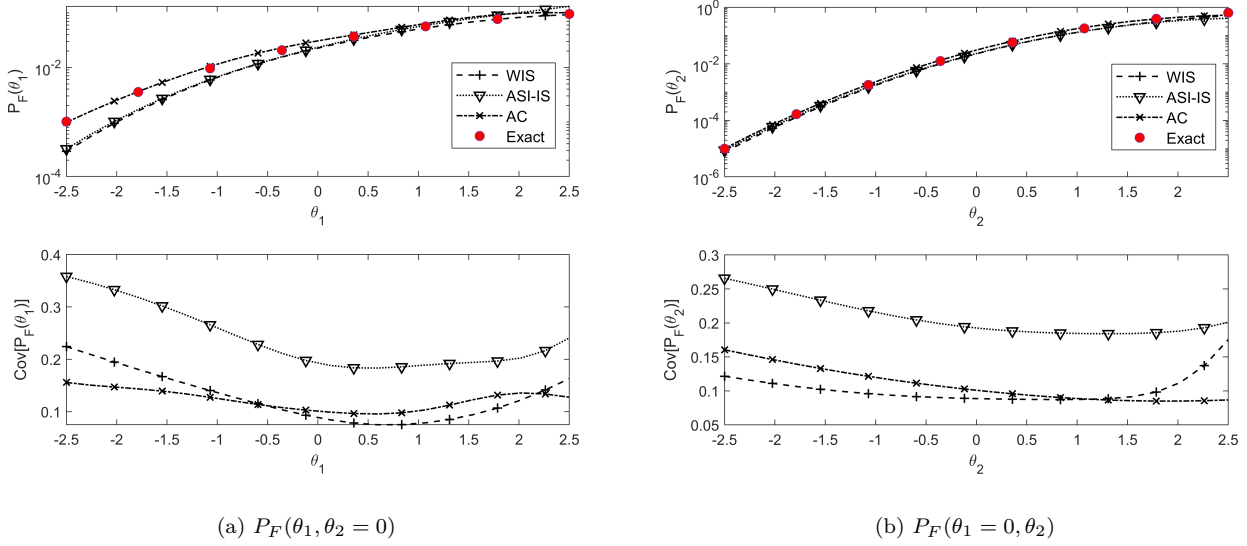


Figure 6: The one-dimensional FPF results by different methods with the same number of simulated samples N_T (Example 1).

Table 1: Average number of samples for different methods under the same stopping criterion (average results over 10 runs) (Example 1).

Methods	Initial design 1	Initial design 2	Initial design 3
WIS	16640	5840	47070
ASI-IS	3470	3010	2578
AC ($N = 100$)	1270	952	1056

308 4.1.3. Parametric Analysis

309 The performance under different settings of the proposed approach is investigated here, i.e.,
 310 with respect to different numbers of samples (N) and initial support parameter points ($\theta_H^{(1)}$). The
 311 proposed approach is carried out considering several repeated runs with a number of samples
 312 from 50 to 500, and different initial support parameter point $\theta_H^{(1)}$, i.e., (1) initial design 1: $\theta_H^{(1)} =$
 313 $[-2.5, -2.5]$, (2) initial design 2: $\theta_H^{(1)} = [0, 0]$, and (3) initial design 3: $\theta_H^{(1)} = [2.5, 2.5]$.

314 Fig. 7 shows the performance of the proposed approach, which gives the total number of
 315 iterations with respect to the number of samples used in each iteration and under different initial

316 support parameter points employing the proposed approach. It can be seen that, (1) when the
 317 number of samples N increases, the number of iterations k decreases, but the number of simulation
 318 samples generated by WIS (denoted as N_T) increases; (2) the total number of evaluations of the
 319 performance function N_{all} is first smooth when N is over about 50 to 400 and then increases when
 320 $N > 400$. Note that N_{all} includes both the simulation samples and the computational cost of
 321 solving the design point in each iteration. In this example, the design point is solved at cost of
 322 about 30 to 100 evaluations of the performance function.

323 It is concluded that the selection of N affects the efficiency of the proposed method. First,
 324 it is recommended N is selected according to the stopping criterion, e.g., if $Cov[\hat{P}_F(\boldsymbol{\theta})] < 0.2$
 325 is expected, then N should be large enough to ensure $Cov[\hat{P}_F^{(i)}(\boldsymbol{\theta}_H^{(i)})] < 0.2$. Second, the other
 326 relevant factor that needs to be considered is the computational cost of solving the design point
 327 involved in the each iteration. It is also recommended that the number of samples N should
 328 be larger than the number of calls in solving the design point of the performance function, thus
 329 leading to a smaller overall computational cost.

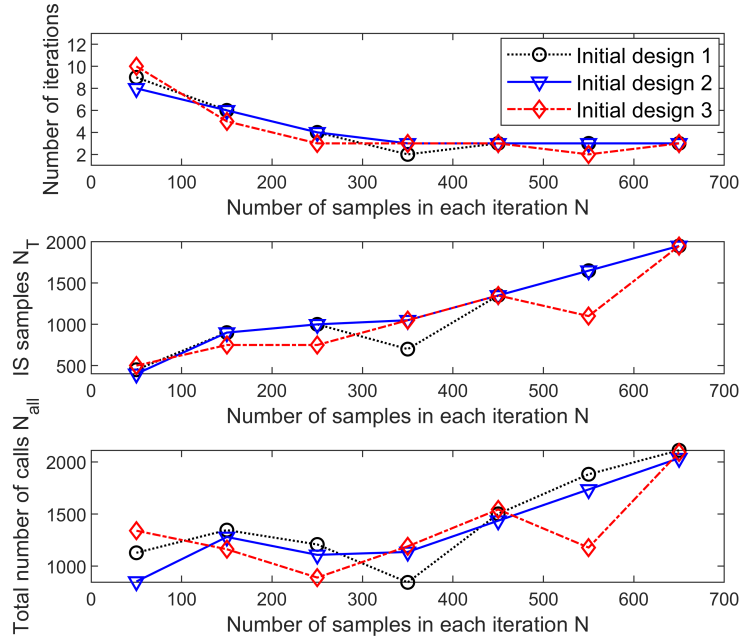


Figure 7: The performance of the the proposed approach with respect to the number of samples used in each iteration and different initial designs (Example 1).

330 4.1.4. Convergence Analysis

331 In this subsection, it will be shown that while the results of the proposed AC are biased, this
 332 bias is sufficiently small. In this test example, for each value of the distribution parameter vector
 333 θ , two independent runs of WIS are carried out, one of which is used for producing the local FPF
 334 estimator $\hat{P}_F^{(i)}(\theta)$ and the other is used solely for determining the weights $w_{(i)}(\theta)$ by means of
 335 Eq. (15). By following this approach, the obtained estimator will become immediately unbiased,
 336 because the weights are determined using samples which are different (completely independent)
 337 from those used for calculating $\hat{P}_F^{(i)}(\theta)$. This approach is denoted as ‘AC(independent)’.

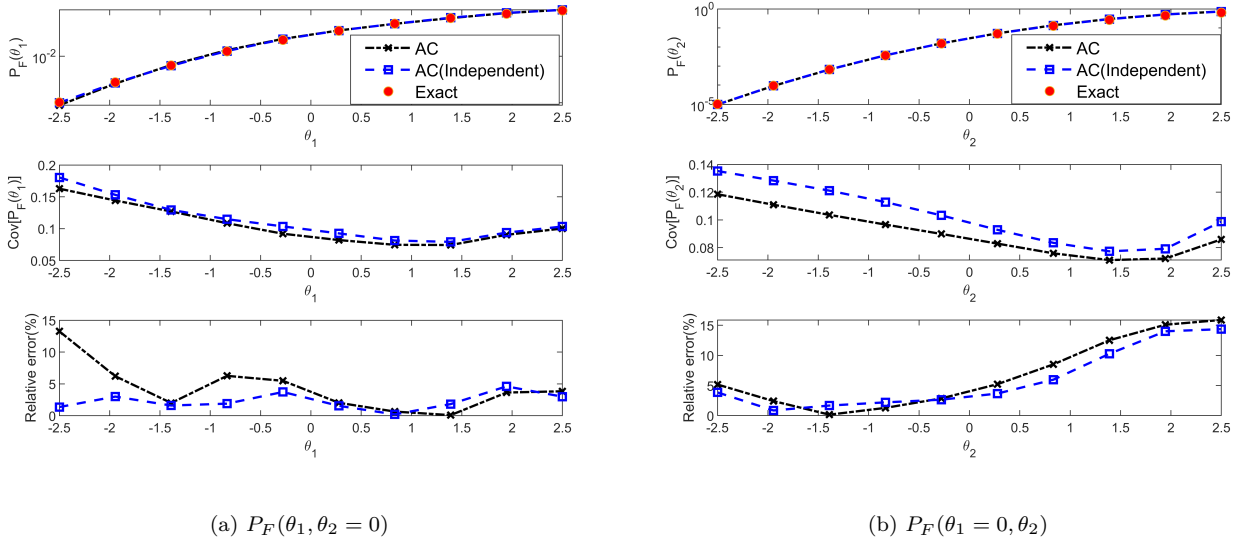


Figure 8: The one-dimensional FPF results by the proposed AC and AC(independent) when $N = 100$ (Example 1).

338 Fig. 8 shows the obtained results in one dimension when $N = 100$. The C.o.V. and relative
 339 error $\epsilon(\theta) = \frac{|\hat{P}_F(\theta) - P_F^{exact}(\theta)|}{P_F^{exact}(\theta)}$ where $P_F^{exact}(\theta)$ is the exact value calculated by MCS. AC takes a
 340 number of $k = 7$ iterations to converge. AC(independent) uses the same information (support
 341 parameter points and component FPF estimators) but calculating the weights through a different
 342 WIS in each iteration. It can be seen from the figure that the results produced with the unbiased
 343 estimator through AC(independent) are almost the same as those of the biased estimator through
 344 AC.

345 4.2. Example 2: Thermal Stress Analysis of Jet Engine Turbine Blade

346 The second example considers a jet engine turbine blade, as shown in Fig. 9. This blade
 347 has interior cooling ducts, through which the flow of cool air maintains the temperature of the

348 blade within the limit for its material. The turbine is a radial array of blades typically made of
 349 nickel alloys. These alloys resist the extremely high temperatures of the gases. At such tempera-
 350 tures, the material expands significantly, producing mechanical stress in the joints and significant
 351 deformations of several millimetres. To avoid mechanical failure and friction between the tip of
 352 the blade and the turbine casing, the blade design must account for the mechanical stresses and
 353 deformations. Failure is defined as the maximum von Mises stress of the structure exceeding the
 354 given allowable value $\sigma_a = 1.5\text{GPa}$, and the corresponding limit state function is:

$$g(\mathbf{x}) = \sigma_a - \sigma_{max}(\mathbf{x}) \quad (20)$$

355 where $\sigma_{max}(\mathbf{x})$ is the maximum von Mises stress of the blade caused by the combination of thermal
 356 and pressure effects; $\mathbf{x} = [E, \lambda, \gamma_{CTE}, P_1, P_2, K_{app}, T_1, T_2]$ is the vector of basic random variables;
 357 E , λ , γ_{CTE} and K_{app} are the Young's modulus, Poisson's ratio, coefficient of thermal expansion
 358 and the thermal conductivity for nickel-based alloy (NIMONIC 90), respectively; P_1 and P_2 are
 359 the pressure loads on the pressure and suction sides of the blade which is due to the high-pressure
 360 gas surrounding these sides of the blade; T_1 is the temperature of the interior cooling air and
 361 T_2 is the temperature on the pressure and suction sides. All these variables are assumed to be
 362 independent truncated normal random variables and their distribution parameters are given in
 363 Table 2.

364 There are three distribution parameters which are of interest in this example, namely $\boldsymbol{\theta} =$
 365 $[\mu_E, \mu_{\gamma_{CTE}}, \mu_{T_2}]$, which are the mean values of E , γ_{CTE} and T_2 . These parameters are contained
 366 within the sets $\theta_1 \in [170, 290]$ (GPa), $\theta_2 \in [10, 18]$ (1/K) and $\theta_3 \in [700, 1300]$ (°C), respectively.

367 The proposed approach is applied to estimate the global FPF of this problem, which is a three-
 368 dimensional function. For this purpose, the initial support point is selected as $\boldsymbol{\theta}_H^{(1)} = [170, 10, 700]$
 369 which corresponds to the lower bound of the design region. Then, $N = 300$ is set for construct-
 370 ing each local estimate of the FPF through Weighted Importance Sampling (WIS) considering
 371 the support point $\boldsymbol{\theta}_H^{(i)}$ which is selected according to the active learning scheme. Traditional Im-
 372 portance Sampling (IS) is adopted to estimate the point-wise failure probability with $N = 1000$
 373 samples for each simulation run. The results from Importance Sampling as regarded as the 'Exact'
 374 values. The proposed scheme combining an adaptive strategy and combination (denoted as AC) is
 375 compared with Weighted Importance Sampling (denoted as WIS) and Augmented Space Integral
 376 using Importance Sampling (denoted as ASI-IS). When performing comparisons, the same number
 377 of simulations is considered for each approach.

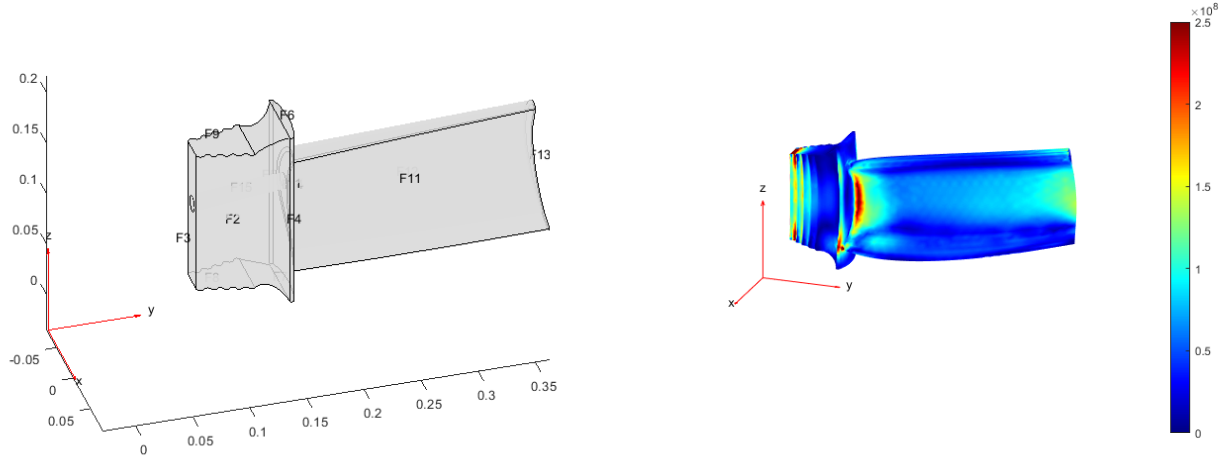


Figure 9: The geometry and von Mises stress of a turbine blade (Example 2).

Table 2: The distribution information of the basic random variables (Example 2).

Random variable	Mean value	Standard deviation
$E(\text{GPa})$	$\theta_1 = \mu_E \in [170, 290]$	23
$\gamma_{CTE}(10^{-6})(1/\text{K})$	$\theta_2 = \mu_{\gamma_{CTE}} \in [10, 18]$	1.4
λ	0.27	0.027
$P_1(\text{kPa})$	500	50
$P_2(\text{kPa})$	450	45
$K_{app}(\text{W/m/K})$	11.5	1.15
$T_1(^{\circ}\text{C})$	150	15
$T_2(^{\circ}\text{C})$	$\theta_3 = \mu_{T_2} \in [700, 1300]$	100

378 Fig. 10 shows the one-dimensional FPF results obtained by different methods, as well as the
379 ‘Exact’ values. It is noticed that the FPF increases with all the design parameters, i.e., the mean
380 values of Young’s modulus, coefficient of thermal expansion and the temperature on the pressure
381 and suction sides. It can be seen from Fig. 10a that the maximum of C.o.V. value by the proposed
382 approach (AC) is less than $c_{tol} = 0.2$, while those associated with WIS and ASI-IS possess larger
383 maximum C.o.V. values. Though the C.o.V. by the proposed AC is not necessarily the smallest
384 among these methods for all θ_1 over the whole design region, the maximum value of C.o.V. is
385 the smallest. In this sense, the proposed approach can obtain more smooth and consistent results
386 under the same computational cost (in terms of the number of samples). The same phenomenon
387 can also be seen in both Figs. 10b and 10c. The effectiveness and advantages of the proposed
388 approach have been demonstrated through this three-dimensional FPF problem.

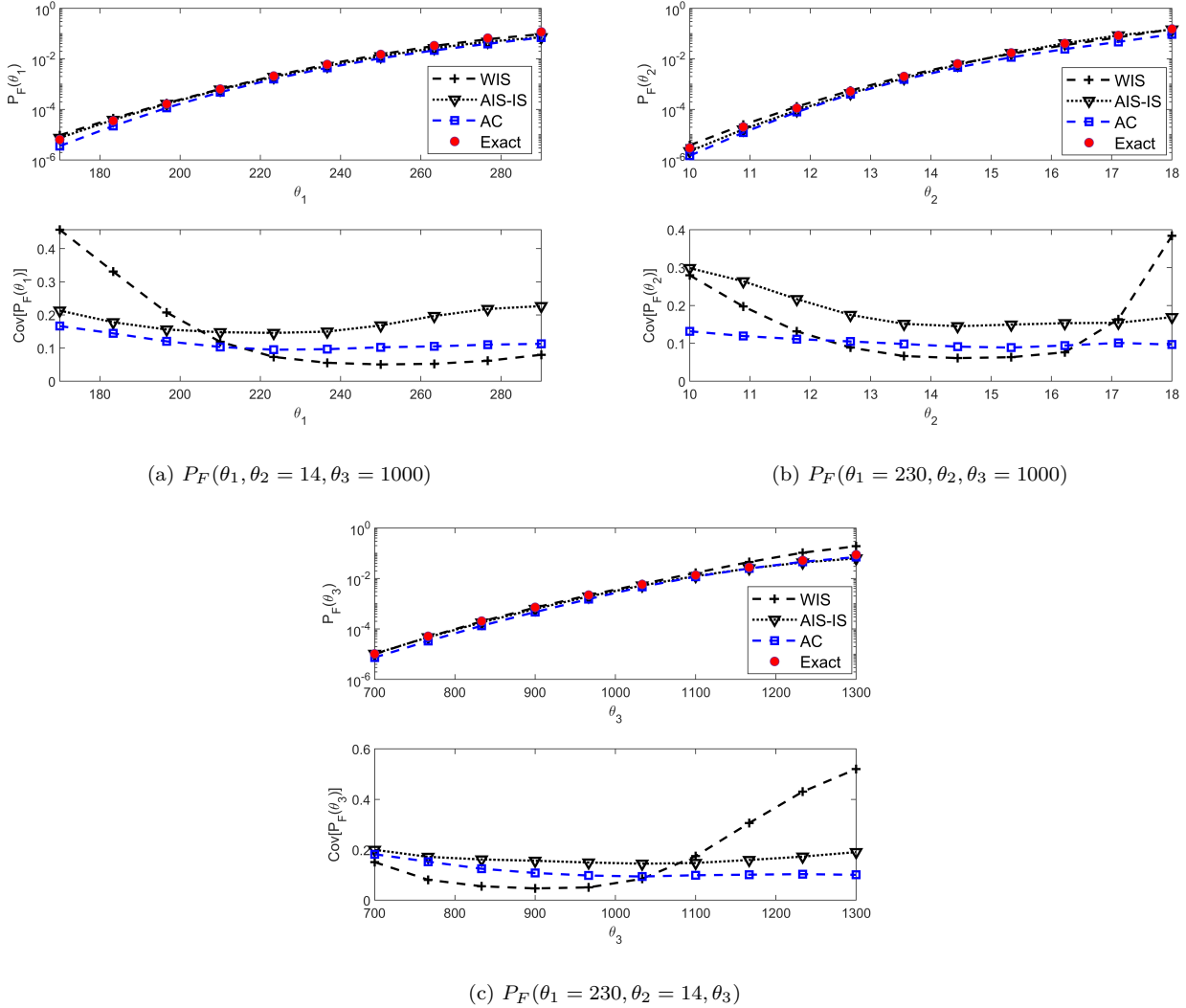


Figure 10: The one-dimensional FPF results by different methods (Example 2).

389 *4.3. Example 3: Shear-beam oscillator*

390 This example is taken from [27] and has been adjusted for the purposes of this work. In this
 391 example, a ten-degree-of-freedom shear-beam oscillator is considered, in which the effects of the
 392 uncertainties in both the system parameters and loading are included. The governing equation is
 393 given by:

$$\mathbf{M}\ddot{\mathbf{u}}(t) + \mathbf{C}\dot{\mathbf{u}}(t) + \mathbf{K}\mathbf{u}(t) = \mathbf{F}(t) \quad (21)$$

394 where

$$\mathbf{M} = \begin{bmatrix} m_1 & 0 & \cdots & 0 \\ 0 & m_2 & \cdots & 0 \\ \cdot & \cdot & \cdots & 0 \\ 0 & \cdots & 0 & m_{10} \end{bmatrix} \quad (22)$$

$$\mathbf{C} = \begin{bmatrix} c_1 + c_2 & -c_2 & \cdots & 0 \\ -c_2 & c_2 + c_3 & \cdots & 0 \\ \cdot & \cdot & \cdots & \cdot \\ 0 & 0 & -c_{10} & c_{10} \end{bmatrix} \quad (23)$$

$$\mathbf{K} = \begin{bmatrix} k_1 + k_2 & -k_2 & \cdots & 0 \\ -k_2 & k_2 + k_3 & \cdots & 0 \\ \cdot & \cdot & \cdots & \cdot \\ 0 & 0 & -k_{10} & k_{10} \end{bmatrix} \quad (24)$$

395 represent the mass, damping and stiffness matrices, respectively, and the random excitation has
 396 the form $\mathbf{F}(t) = p(t) \cdot [m_1, \cdots, m_{10}]^T$, with T indicating transpose of the argument. The random
 397 excitation possesses duration $T = 20$ s and its discretization interval is $\Delta t = 0.05$ s. The values
 398 of the base random excitation at a given number of time steps constitute the vector of random
 399 parameters. Thus, there are $n_T = T/\Delta t = 401$ input random variables to discretise the excitation
 400 $\mathbf{F}(t)$ at time instants $t_k = (k - 1)\Delta t$ ($k = 1, 2, \dots, n_T$). It is assumed that the mass parameters
 401 m_1, \cdots, m_{10} and stiffness parameters k_1, \cdots, k_{10} and ξ_1, \cdots, ξ_{10} are all independent (truncated)
 402 Gaussian random variables with mean values of $\mu_{m_i} = 10\text{Mg}$, μ_{k_i} (design parameter), and $\mu_{\xi_i} =$
 403 0.04 . The standard deviations for these variables are listed in Table 3. It is also assumed that
 404 $c_i = 2 \xi_i \sqrt{m_i k_i}$ ($i = 1, 2, \dots, 10$).

405 The uncertain excitation is modelled by a modulated filtered Gaussian white noise as follows:

$$p(t) = \omega_1^2 v_1 + 2\omega_1 \zeta_1 \dot{v}_1 - \omega_2^2 v_2 - 2\omega_2 \zeta_2 \dot{v}_2 \quad (25)$$

406 where

$$\frac{d}{dt} \begin{bmatrix} v_1 \\ \dot{v}_1 \\ v_2 \\ \dot{v}_2 \end{bmatrix} = \begin{bmatrix} 0 & 1 & 0 & 0 \\ -\omega_1^2 & -2\omega_1\zeta_1\dot{v}_1 & 0 & 0 \\ 0 & 0 & 0 & 1 \\ \omega_2^2 & 2\omega_1\zeta_1\dot{v}_1 & -\omega_2^2 & -2\omega_2\zeta_2\dot{v}_2 \end{bmatrix} \begin{bmatrix} v_1 \\ \dot{v}_1 \\ v_2 \\ \dot{v}_2 \end{bmatrix} + \begin{bmatrix} 0 \\ w(t) \\ 0 \\ 0 \end{bmatrix} \quad (26)$$

407 where $w(t)$ is Gaussian white noise with the autocorrelation function $E[w(t)w(t+\tau)] = I\delta(\tau)h^2(t)$
 408 in which I denotes the intensity of the white noise, $\delta(\cdot)$ is the Dirac delta and $h(\cdot)$ is an envelope
 409 function defined as:

$$h(t) = \begin{cases} 0 & t \leq 0 \text{ s} \\ t/2 & 0 \text{ s} \leq t \leq 2 \text{ s} \\ 1 & 2 \text{ s} \leq t \leq 10 \text{ s} \\ \exp[-0.1(t - 10)] & t \geq 10 \text{ s} \end{cases} \quad (27)$$

410 The values $\omega_1 = 15.0 \text{ rad/s}$, $\zeta_1 = 0.8$, $\omega_2 = 0.3 \text{ rad/s}$, $\zeta_2 = 0.995$, and $I = 0.08 \text{ m}^2/\text{s}^3$ are
 411 used to model the filter. Failure is defined as an event where the relative displacement of the first
 412 degree of freedom exceeds 0.06 m, and the limit state function given by

$$g(\mathbf{x}, \mathbf{z}) = b - \max_{j=1}^{n_T} (|Y_{1j}(\mathbf{x}, \mathbf{z})|) \quad (28)$$

413 where $b=0.06 \text{ m}$; Y_{1j} denotes the structural response of the first degree of freedom at time step j ;
 414 $\mathbf{x} = [x_1, x_2, \dots, x_n]$ is the vector of the random variables associated with the structural parameters;
 415 $\mathbf{z} = [z_1, z_2, \dots, z_{n_t}]$ is the vector of the random variables used to characterise the stochastic
 416 excitation, which are assumed as i.i.d. standard Gaussian variables in this contribution; and b_i is
 417 the i -th threshold level.

Table 3: The distribution information of the basic structural random variables (Example 3).

Random variable	Mean value	Standard deviation
$k_1(\text{MN/m})$	$\theta = \mu_{k_1} \in [20, 60]$	4
$k_i(i = 2, \dots, 10)(\text{MN/m})$	40	4
$m_i(i = 1, \dots, 10)(\text{Mg})$	10	0.5
$\xi_i(i = 2, \dots, 10)$	0.04	0.008

418 In this example, the mean stiffness μ_{k_1} is taken as the design parameter, i.e., $\theta = \mu_{k_1}$ for which
419 the design region is $\theta = \mu_{k_1} \in [30, 60]\text{MN/m}$.

420 The proposed approach based on adaptive strategy and combination (AC) is applied with
421 $N = 100$, and $c_{tol} = 0.2$. It is found that a total of $k = 9$ iterations are required to achieve conver-
422 gence. Traditional Importance Sampling (IS) is also carried out to obtain the point-wise failure
423 probabilities which are taken as the ‘exact’ values, where 1000 samples are used to estimate each
424 probability value. In addition, the FPF is calculated by means of Weighted Importance Sampling
425 (WIS) and Augmented Space Integral (ASI). Both WIS and ASI are implemented considering a
426 total of $N_T = N \times k = 100 \times 9 = 900$ samples, in order to ensure a fair comparison with the results
427 produced with the proposed approach. The estimates for the FPF obtained with the aforemen-
428 tioned methods are shown in Fig. 11. It is seen that the FPF decreases with respect to the mean
429 value of k_1 . This makes sense from a physical viewpoint, as a larger stiffness helps to control the
430 maximum displacement. While errors exist in the results of WIS and ASI, the proposed approach
431 obtains an accurate result that is consistent with the reference values. Meanwhile, the C.o.V. of
432 FPF estimate by the proposed approach is smooth over the design region and it is always less
433 than 0.2 (which is consistent with the convergence criterion set beforehand). On the contrary, the
434 maximum values of the coefficient of variation associated with WIS and ASI are about 0.4 and
435 0.8, respectively. The advantage of the proposed approach is clearly shown.

436 5. Conclusions

437 This paper presents an efficient approach based on adaptive strategy and combination algo-
438 rithm (AC) for structural global failure probability function (FPF) estimation. It approximates
439 the global FPF by aggregating local estimates of FPF. These local estimates are constructed
440 around support points which are selected in an adaptive manner. Furthermore, these local esti-
441 mates are aggregated optimally according to a prescribed criterion that minimised the coefficient
442 of variation of the global FPF estimate. The local estimation of the FPF is carried out resorting
443 to Weighted Importance Sampling.

444 Through the examples addressed in this contribution, the following conclusions can be made:

- 445 • The proposed adaptive strategy is effective in identifying the design value possessing the
446 largest C.o.V. estimator.

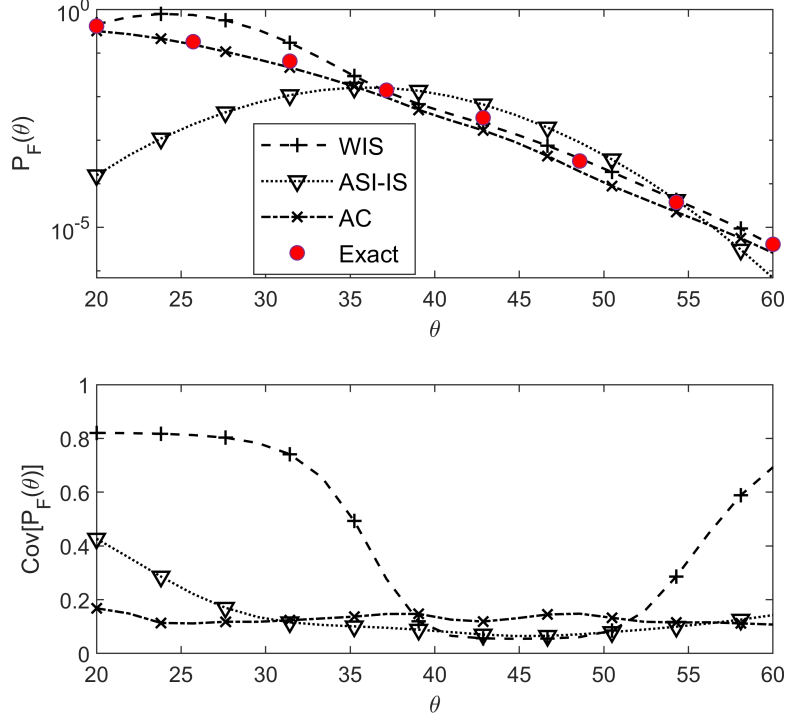


Figure 11: The FPF results by different methods (Example 3).

447

- The proposed optimal combination based on minimising the C.o.V. of the FPF estimate can result in an estimate with a C.o.V. smaller than any of the local FPF estimators.

448

449

- The proposed approach is numerically more efficient than the augmented space integral (ASI) method when both of them use Importance Sampling (IS) as the simulation method.

450

451

- The proposed approach is numerically more accurate than the Weighted Importance Sampling (WIS) when both of them use Importance Sampling (IS) as the simulation method.

452

453

454

455

456

457

458

459

Future research efforts will aim at expanding the scope of application of the proposed framework. For example, one possible path is exploring the assessment of local FPF estimators by means of Weighted Importance Sampling by using an adaptive Importance Sampling Density function. Furthermore, the proposed strategy can be implemented with other simulation strategies for estimating local FPF, such as weighted Monte Carlo Simulation or weighted Subset Simulation. At last, the application of the proposed approach to other problems should be explored as well, such as reliability-based design optimization and imprecise reliability estimation.

460 **Acknowledgements**

461 Xiukai Yuan would like to acknowledge financial support from NSAF (Grant No. U1530122),
 462 the Aeronautical Science Foundation of China (Grant No. ASFC-20170968002).

463 **Appendix A. Selection of Weights in combination algorithm**

464 This Appendix presents detailed deductions for the optimal weights which minimize the C.o.V.
 465 and variance as given by Eqs. (15) and (13), respectively.

466 As the optimization problem of minimizing the $Cov[\hat{P}_{F,C}^k(\boldsymbol{\theta})]$ is equal to minimizing the
 467 $Cov^2[\hat{P}_{F,C}^k(\boldsymbol{\theta})]$, then the optimal weights based on minimizing the C.o.V. can be stated as fol-
 468 lows:

$$\begin{aligned} \min \quad & Cov^2[\hat{P}_{F,C}^k(\boldsymbol{\theta})] = \sum_{i=1}^k w_i^2(\boldsymbol{\theta}) Cov^2[\hat{P}_F^{(i)}(\boldsymbol{\theta})] \\ \text{s.t.} \quad & \sum_{i=1}^k w_i(\boldsymbol{\theta}) = 1 \end{aligned} \quad (\text{A.1})$$

469 This problem can be solved by the method of Lagrange multipliers. The Lagrangian of the
 470 problem in Eq. (A.1) is:

$$L(\mathbf{w}, \lambda) = \sum_{i=1}^k w_i^2(\boldsymbol{\theta}) Cov^2[\hat{P}_F^{(i)}(\boldsymbol{\theta})] + \lambda \left(\sum_{i=1}^k w_i(\boldsymbol{\theta}) - 1 \right) \quad (\text{A.2})$$

471 The first-order necessary conditions for optimality read:

$$\frac{\partial L(\mathbf{w}, \lambda)}{\partial w_i(\boldsymbol{\theta})} = 0, \quad \frac{\partial L(\mathbf{w}, \lambda)}{\partial \lambda} = 0 \quad (\text{A.3})$$

472 Solving this equation will result in the following expressions

$$\begin{aligned} w_i(\boldsymbol{\theta}) &= -\frac{\lambda}{2} Cov^{-2}[\hat{P}_F^{(i)}(\boldsymbol{\theta})] \\ \lambda &= -\frac{2}{\sum_{i=1}^k Cov^{-2}[\hat{P}_F^{(i)}(\boldsymbol{\theta})]} \end{aligned} \quad (\text{A.4})$$

473 which leads to:

$$w_i(\boldsymbol{\theta}) = \frac{Cov^{-2}[\hat{P}_F^{(i)}(\boldsymbol{\theta})]}{\sum_{j=1}^k Cov^{-2}[\hat{P}_F^{(j)}(\boldsymbol{\theta})]} \quad (i = 1, \dots, k) \quad (\text{A.5})$$

474 Since the objective function is convex (quadratic in w) and the constraint is affine, the result of
 475 Eq. (A.5) is the global optimum.

476 Similarly, the optimal weights that minimise the variance can be also obtained by solving the
 477 following optimization problem

$$\begin{aligned} \min \quad & \sum_{i=1}^k w_i^2(\boldsymbol{\theta}) \text{Var}[\hat{P}_F^{(i)}(\boldsymbol{\theta})] \\ \text{s.t.} \quad & \sum_{i=1}^k w_i(\boldsymbol{\theta}) = 1 \end{aligned} \quad (\text{A.6})$$

478 and the cooresponding optimal weights are given by:

$$w_i(\boldsymbol{\theta}) = \frac{\text{Var}^{-1}[\hat{P}_F^{(i)}(\boldsymbol{\theta})]}{\sum_{j=1}^k \text{Var}^{-1}[\hat{P}_F^{(j)}(\boldsymbol{\theta})]} \quad (i = 1, \dots, k) \quad (\text{A.7})$$

479 Appendix B. Convergence of the optimal combination algorithm

480 In this Appendix, we obtain the following lemma for the estimator $\hat{P}_{F,C}^{(k)}(\boldsymbol{\theta})$ in Eq. (2) associated
 481 with the proposed optimal combination algorithm.

482 *Lemma 1.* Provided that $\text{Cov}[\hat{P}_F^{(j)}(\boldsymbol{\theta})]$ is finite, the estimator $\hat{P}_{F,C}^{(k)}(\boldsymbol{\theta})$ in Eq.(2) converges to
 483 $P_F(\boldsymbol{\theta})$ when N goes to infinity.

484 As $\hat{P}_F^{(i)}(\boldsymbol{\theta})$ is unbiased for each $i = 1, \dots, k$, thus according to the central limit theory, we have

$$\lim_{N \rightarrow +\infty} \hat{P}_F^{(i)}(\boldsymbol{\theta}) = P_F(\boldsymbol{\theta}) \quad (\text{B.1})$$

When N goes to infinity,

$$\lim_{N \rightarrow +\infty} \hat{P}_{F,C}^{(k)}(\boldsymbol{\theta}) = \lim_{N \rightarrow +\infty} \sum_{i=1}^k w_i(\boldsymbol{\theta}) \hat{P}_F^{(i)}(\boldsymbol{\theta}) = \sum_{i=1}^k \lim_{N \rightarrow +\infty} w_i(\boldsymbol{\theta}) P_F(\boldsymbol{\theta}) \quad (\text{B.2})$$

And according to Eqs. (10) and (B.1), the limit of the weights in Eq.(B.2) becomes

$$\lim_{N \rightarrow +\infty} w_i(\boldsymbol{\theta}) = \lim_{N \rightarrow +\infty} \frac{\text{Cov}^{-2}[\hat{P}_F^{(i)}(\boldsymbol{\theta})]}{\sum_{j=1}^k \text{Cov}^{-2}[\hat{P}_F^{(j)}(\boldsymbol{\theta})]} = \frac{P_F^2(\boldsymbol{\theta}) \lim_{N \rightarrow +\infty} \text{Var}^{-1}[\hat{P}_F^{(i)}(\boldsymbol{\theta})]}{\sum_{j=1}^k P_F^2(\boldsymbol{\theta}) \lim_{N \rightarrow +\infty} \text{Var}^{-1}[\hat{P}_F^{(j)}(\boldsymbol{\theta})]} \quad (\text{B.3})$$

$$= \frac{V_i^{-1}}{\sum_{j=1}^k V_j^{-1}} \quad (\text{B.4})$$

where

$$V_i = \lim_{N \rightarrow +\infty} \left\{ \frac{1}{N} \sum_{j=1}^N \left[\frac{I_F(\mathbf{x}^{(j)}) f(\mathbf{x}^{(j)} | \boldsymbol{\theta})}{H(\mathbf{x}^{(j)} | \mathbf{x}^{*(i)})} \right]^2 - [\hat{P}_F^{(i)}(\boldsymbol{\theta})]^2 \right\} \quad (\text{B.5})$$

$$= \left\{ \int \left[\frac{I_F(\mathbf{x}) f(\mathbf{x} | \boldsymbol{\theta})}{H(\mathbf{x} | \mathbf{x}^{*(i)})} \right]^2 H(\mathbf{x} | \mathbf{x}^{*(i)}) d\mathbf{x} - [P_F(\boldsymbol{\theta})]^2 \right\} \quad (\text{B.6})$$

485 It is known that $H(\mathbf{x}|\mathbf{x}^{*(i)}) \neq \frac{I_F(\mathbf{x})f(\mathbf{x}|\boldsymbol{\theta})}{P_F(\boldsymbol{\theta})}$ as it is based on design point $\mathbf{x}^{*(i)}$, then $V_i > 0$. Thus
 486 $\sum_{i=1}^k \lim_{N \rightarrow +\infty} w_i(\boldsymbol{\theta}) = 1$ also holds. Lemma 1 can be derived straightforwardly by rewriting
 487 above Eq. (B.2) as

$$\lim_{N \rightarrow +\infty} \hat{P}_{F,C}^{(k)}(\boldsymbol{\theta}) = P_F(\boldsymbol{\theta}) \sum_{i=1}^k \lim_{N \rightarrow +\infty} w_i(\boldsymbol{\theta}) = P_F(\boldsymbol{\theta}) \quad (\text{B.7})$$

488 Note that Eq. (B.7) does not hold for an extreme case, e.g., $Cov \left[\hat{P}_F^{(j)}(\boldsymbol{\theta}) \right]$ is infinite. Thus, in
 489 practical computation, these extreme cases should be taken care.

490 References

- 491 [1] M. Faes, D. Moens, Recent trends in the modeling and quantification of non-probabilistic
 492 uncertainty, *Archives of Computational Methods in Engineering* 27 (2020) 633–671.
- 493 [2] M. A. Valdebenito, H. A. Jensen, H. Hernandez, L. Mehrez, Sensitivity estimation of failure
 494 probability applying line sampling, *Reliability Engineering & System Safety* 171 (2018) 99–
 495 111.
- 496 [3] M. A. Valdebenito, G. I. Schuëller, A survey on approaches for reliability-based optimization,
 497 *Structural and Multidisciplinary Optimization* 42 (2010) 645–663.
- 498 [4] M. Gasser, G. I. Schuëller, Reliability-based optimization of structural systems, *Mathematical*
 499 *Methods of Operations Research* 46 (1997) 287–307.
- 500 [5] H. A. Jensen, Structural optimization of linear dynamical systems under stochastic excita-
 501 tion: a moving reliability database approach, *Computer methods in applied mechanics and*
 502 *engineering* 194 (2005) 1757–1778.
- 503 [6] M. Li, M. Sadoughi, Z. Hu, C. Hu, A hybrid gaussian process model for system reliability
 504 analysis, *Reliability Engineering & System Safety* 197 (2020) 106816.
- 505 [7] M. I. Radaideh, T. Kozłowski, Surrogate modeling of advanced computer simulations using
 506 deep gaussian processes, *Reliability Engineering & System Safety* 195 (2020) 106731.
- 507 [8] C. Cortes, V. Vapnik, Support-vector networks, *Machine learning* 20 (1995) 273–297.
- 508 [9] Y. Wang, X. Yu, X. Du, Improved reliability-based optimization with support vector machines
 509 and its application in aircraft wing design, *Mathematical Problems in Engineering* 2015
 510 (2015).

- 511 [10] B. Echard, N. Gayton, M. Lemaire, Ak-mcs: an active learning reliability method combining
512 kriging and monte carlo simulation, *Structural Safety* 33 (2011) 145–154.
- 513 [11] Q. Pan, D. Dias, An efficient reliability method combining adaptive support vector machine
514 and monte carlo simulation, *Structural Safety* 67 (2017) 85–95.
- 515 [12] T. Zou, S. Mahadevan, A direct decoupling approach for efficient reliability-based design
516 optimization, *Structural and Multidisciplinary Optimization* 31 (2006) 190.
- 517 [13] X. Yuan, Local estimation of failure probability function by weighted approach, *Probabilistic*
518 *Engineering Mechanics* 34 (2013) 1–11.
- 519 [14] X. Yuan, Z. Zheng, B. Zhang, Augmented line sampling for approximation of failure probabil-
520 ity function in reliability-based analysis, *Applied Mathematical Modelling* 80 (2020) 895–910.
- 521 [15] S. Au, Reliability-based design sensitivity by efficient simulation, *Computers & structures*
522 83 (2005) 1048–1061.
- 523 [16] J. Ching, Y.-H. Hsieh, Local estimation of failure probability function and its confidence
524 interval with maximum entropy principle, *Probabilistic Engineering Mechanics* 22 (2007)
525 39–49.
- 526 [17] J. Ching, Y.-H. Hsieh, Approximate reliability-based optimization using a three-step ap-
527 proach based on subset simulation, *Journal of engineering mechanics* 133 (2007) 481–493.
- 528 [18] A. A. Taflanidis, J. L. Beck, Stochastic subset optimization for reliability optimization and
529 sensitivity analysis in system design, *Computers & Structures* 87 (2009) 318–331.
- 530 [19] K. Feng, Z. Lu, C. Ling, W. Yun, An innovative estimation of failure probability function
531 based on conditional probability of parameter interval and augmented failure probability,
532 *Mechanical Systems and Signal Processing* 123 (2019) 606–625.
- 533 [20] C. Ling, Z. Lu, X. Zhang, An efficient method based on ak-mcs for estimating failure prob-
534 ability function, *Reliability Engineering & System Safety* 201 (2020) 106975.
- 535 [21] X. Yuan, S. Liu, M. A. Valdebenito, J. Gu, M. Beer, Efficient framework for failure probability
536 function estimation in augmented space, *Structural Safety* 92 (2021) 102104.

- 537 [22] H. Zhang, C. Zhou, H. Zhao, Z. Zhang, An ensemble model-based method for estimat-
538 ing failure probability function with application in reliability-based optimization, *Applied*
539 *Mathematical Modelling* 108 (2022) 445–468.
- 540 [23] A. Tabandeh, G. Jia, P. Gardoni, A review and assessment of importance sampling methods
541 for reliability analysis, *Structural Safety* 97 (2022) 102216.
- 542 [24] R. Melchers, Importance sampling in structural systems, *Structural safety* 6 (1989) 3–10.
- 543 [25] I. Papaioannou, D. Straub, Combination line sampling for structural reliability analysis,
544 *Structural Safety* 88 (2021) 102025.
- 545 [26] A. M. Hasofer, N. C. Lind, Exact and invariant second-moment code format, *Journal of the*
546 *Engineering Mechanics division* 100 (1974) 111–121.
- 547 [27] G. I. Schuëller, H. J. Pradlwarter, Benchmark study on reliability estimation in higher
548 dimensions of structural systems—an overview, *Structural Safety* 29 (2007) 167–182.